Gain-Scheduling H_∞ Control of the Launcher in Atmospheric Flight via Linear-Parameter Varying Techniques

Olivier Voinot[*], *Pierre Apkarian*[†], *Daniel Alazard*[‡]

Résumé

This paper is concerned with the design of a gain-scheduled controller for the attitude control of a launcher in atmospheric flight. The design problem is characterized by classical requirements such as satisfactory phase/gain margin constraints and flexible modes attenuation as well as time-domain constraints in the form of an upper bound on the angle of attack in the presence of wind disturbance. Moreover, these requirements must be fulfilled over the full atmospheric flight.

In order to achieve this goal, we exploit a recently available Linear Parameter-Varying (LPV) technique suitably extended to discrete-time systems. The advantage of this technique is that both time-invariant constraints and the gain-scheduling phase are incorporated into a single design procedure and neither interpolation nor extensive simulations are required to accomplish the overall design task.

An important ingredient in the proposed technique is the Cross Standard Form formulation which allows to incorporate the various specifications of the launcher problem in a streamlined manner. It leads to a specific control standard form which can be immediately handled by the LPV design technique under consideration.

Keywords : multi-objective synthesis, performance, robustness, Cross Standard Form, launcher, gain scheduling

[*]ONERA-CERT, Control System Dept., 2 av. Edouard Belin, 31055 Toulouse, FRANCE - Email : `voinot@cert.fr`, http://www.cert.fr/dcsd/cdin/voinot/

[†]ONERA-CERT, Control System Dept., 2 av. Edouard Belin, 31055 Toulouse, FRANCE - Email : `apkarian@cert.fr`, http://www.cert.fr/dcsd/cdin/apkarian/

[‡]SUPAERO, 10 av. Edouard Belin - BP. 4032, 31055 Toulouse, FRANCE - Email : `alazard@supaero.fr`, http://www.supaero.fr/page-perso/autom/alazard

1 Introduction

In this paper,we consider the low-level control loop of a non-stationary launcher during atmospheric flight. Only the yaw attitude is explored: the problem is formulated in terms of angle of attack regulation in face of a typical wind profile (disturbance rejection problem) and consumption reduction. Robustness specifications are expressed in the frequency domain for a set of operating instants regularly spaced along the flight path: the open loop transfer ($L(s) = K(s)G(s)$) must satisfy templates on the Nichols chart for various critical configurations sampled in the uncertain parameter space. Uncertain parameters are the main dynamic parameters on the rigid mode (aerodynamic coefficient, thruster efficiency,...) and on the bending modes (natural pulsations, modal participation factors).

With respect to the pure stationary synthesis problem at one flight instant, there is no methods, to our knowledge, that can handle a set of specifications (time-domain performance and open-loop frequency-domain specifications) in a streamlined manner. Although our approach is also indirect, its capability to take advantage of know-how is particularly highlighted in this application: the time-domain performance specification (angle-of-attack peak amplitude in response to typical wind profiles) is handled by a non-conventional LQG synthesis in which the LQ state feedback is computed in a two-step procedure based on physical considerations. Then, this synthesis is incorporated into a standard H_∞ problem in order to meet frequency-domain templates. The final H_∞ synthesis meets all the specifications and produces a low-order compensator in regard to alternative approaches applied on the same problem ([1, 2, 3]). Our method is based on the CSF (Cross Standard Form) [4] presented as a generalization of the LQ inverse problem to the H_2 and H_∞ inverse problem. The CSF allows to formulate a standard problem from which an initial compensator can be obtained by H_2 or H_∞ synthesis. The CSF is used to mix various synthesis techniques in order to satisfy the different specifications of the launcher control problem. Indeed, the general idea is to perform a first synthesis to reach some specifications, mainly performance specifications. Then, the CSF is applied to this first solution to initialize a standard problem which will be gradually completed to handle frequency-domain or parametric robustness specifications.

Considering the non-stationary problem, we design the LTV plant as a linear interpolation of the H_∞ problems of control constructed for different points on the flight envelope. We use a linear interpolation, because the LTV model of the launcher is the result of a linear interpolation of the physical parameters. The construction of the H_∞ problems presented in this paper is the discrete-time version of the method proposed in our previous paper [4]. This discrete-time version produce a simpler control law. Given the LTV model of the launcher, the overall control law is designed using the LPV synthesis technique introduced in [5] suitably extended to discrete-time systems. Hence the full launcher flight envelope is dealt with in a single phase which overcomes the need for repeated syntheses and simulations.

The paper is structured as follows. Some notations and prerequisites are introduced in Section 2. Section 3 is devoted to the characterization and the construction of gain-scheduled controllers. In Section 4, we briefly discuss the CSF concept which is used in the launcher control problem. The launcher control problem considered in this paper and described Section 5 is the same as presented in [3] and [1]. Section 6 is devoted to the standard form construction and its use to merge together the various design specifications. Finally, Section 7 discuses the results obtained through the proposed methodology.

2 Notations and State-Space Setup

The notation used in the paper is fairly conventional.

A^T	Transposed of matrix A
$\dot{x}$	Time derivation ($\dot{x} = dx/dt$)
s	LAPLACE variable
T_s	Sampling period
x_k or $x(k)$	Discrete-time value of x ($x(t)\|_{t=kT_s}$)
z^{-1}	delay operator
$G(\delta) := \left[\begin{array}{c\|c} A & B \\ \hline C & D \end{array}\right]$	state-space realization of transfer $G(\delta)$: $G(\delta) = D + C(\delta I - A)^{-1}B$ ($\delta = s$ or z)

For real symmetric matrices M, $M > 0$ stands for "positive definite" and means that all the eigenvalues of M are positive. Similarly, $M < 0$ means "negative definite" (all the eigenvalues of M are negative) and $M \geq 0$ stands for "nonnegative definite" (the smallest eigenvalue of M is nonnegative). We shall also use the LFT notation. For appropriately dimensioned matrices K and $M = \begin{bmatrix} M_{11} & M_{12} \\ M_{21} & M_{22} \end{bmatrix}$ and assuming the inverses exist, the upper LFT is defined as

$$F_u(M, K) = M_{22} + M_{21}K(I - M_{11}K)^{-1}M_{12}. \tag{1}$$

Similarly, the lower LFT is defined as

$$F_l(M, K) = M_{11} + M_{12}K(I - M_{22}K)^{-1}M_{21}. \tag{2}$$

The L_2 norm of a signal $w(t)$ on $[0, \infty)$ is defined as

$$\|w\|_{L_2}^2 := \int_0^\infty w(t)^T w(t) dt \text{ or } \sum_{k=0}^{\infty} w(kT)^T w(kT) \ .$$

Acronyms

CSF	Cross Standard Form
LFT	Linear Fractional Transformation
LPV	Linear Parameter-Varying
LQ	Linear Quadratic
LQG	Linear Quadratic Gaussian
LTI	Linear Time Invariant
LTR	Loop Transfer Recovery
LTV	Linear Time-Varying

3 Output-Feedback Synthesis

In this section we recap some known results on the LPV gain-scheduling technique with bounded parameter variations rates. The reader is referred to [5] for a detailed discussion on this technique and also to references [6, 7, 8] for details, insights and applications of analogous gain-scheduling techniques.

The problem addressed by this technique is the following. Suppose we are given an LPV plant $G(\theta)$ with state-space realization

$$\begin{array}{lcl} x_{k+1} & = & A(\theta)x_k + B_1(\theta)w_k + B_2(\theta)u_k \\ z_k & = & C_1(\theta)x_k + D_{11}(\theta)w_k + D_{12}(\theta)u_k \\ y_k & = & C_2(\theta)x_k + D_{21}(\theta)w_k \ , \end{array} \tag{3}$$

where

$$A \in \mathbb{R}^{n\times n}, \quad D_{12} \in \mathbb{R}^{p_1\times m_2}, \text{and} \quad D_{21} \in \mathbb{R}^{p_2\times m_1}$$

define the problem dimension. The time-varying parameter $\theta_k := (\theta_1, \cdots, \theta_L)^T$ is assumed bounded as follows,

— each parameter θ_i ranges between known extremal values $\underline{\theta}_i$ and $\bar{\theta}_i$:

$$\theta_i \in [\underline{\theta}_i, \bar{\theta}_i], \qquad \forall k \geq 0\,. \tag{4}$$

The first assumption means that the parameter vector θ is valued in a hypercube Θ. An important assumption made throughout is the following:

(A1) We will assume throughout that the evolutions of the system are well modeled by a sequence of LTI systems. Therefore, the scheduling variable θ is time-invariant. This somewhat surprising assumption is motivated by the fact that the launcher is a mildly non-stationary system and most design specfications are of time-invariant nature (gain/phase margins, flexible modes attenuation, etc.). The design problem is thus based on a sequence of linear models along the trajectory of the launcher. We will however keep the terminology LPV system or LPV design with a slight abuse.

With these definitions in mind, the gain-scheduled output-feedback control problem consists of finding a dynamic LPV controller, $K(\theta)$, with state-space equations

$$\begin{array}{lcl} x_K(k+1) & = & A_K(\theta)x_K(k) + B_K(\theta)y(k) \\ u(k) & = & C_K(\theta)x_K(k) + D_K(\theta)y(k) \ , \end{array} \tag{5}$$

which ensures internal stability and a minimal L_2-gain bound γ for the closed-loop operator (3)-(5) from the disturbance signal w to the error signal z. Note that A and A_K have the same dimensions, since we restrict the discussion to the full-order case. Denoting $x_{\rm cl}$ the states of the closed-loop system (3)-(5), that is,

$$x_{\rm cl} = \left[\begin{array}{c} x \\ x_K \end{array} \right],$$

the formulation of such controllers can be handled via the Bounded Real Lemma with quadratic parameter-dependent Lyapunov functions $V(x_{\rm cl}, \theta) = x_{\rm cl}^T P(\theta) x_{\rm cl}$ [5]. Note that the controller state-space matrices are allowed to depend explicitly on the derivative of the time-varying parameter θ.

Except the usual smoothness assumptions on the dependence on θ, the problem data and variables will be unrestricted hereafter. The basic characterization of gain-scheduled controllers with guaranteed L_2-gain performance is presented in the next theorem where the dependence of data and variables on θ has been dropped for simplicity.

Theorem 3.1 (Basic Characterization [5]) *Consider the LPV plant governed by (3), with parameter trajectories constrained by (4) and the assumption* **(A1)** *in force. There exists a gain-scheduled output-feedback controller (5) enforcing internal stability and a bound* γ *on the* L_2 *gain of the closed-loop system (3) and (5), whenever there exist parameter-dependent symmetric matrices* Y *and* X *and a parameter-dependent quadruple of state-space data* $(\widehat{A}_K, \widehat{B}_K, \widehat{C}_K, D_K)$ *such that for all* θ *in* Θ *the following infinite-dimensional LMI problem holds,*

$$\begin{bmatrix} -X & * & * & * & * & * \\ -I & -Y & * & * & * & * \\ (XA+\widehat{B}_K C_2)^T & (A+B_2 D_K C_2)^T & -X & * & * & * \\ \widehat{A}_K^T & (AY+B_2\widehat{C}_K)^T & -I & -Y & * & * \\ (XB_1+\widehat{B}_K D_{21})^T & (B_1+B_2 D_K D_{21})^T & 0 & 0 & -\gamma I & * \\ 0 & 0 & C_1+D_{12}D_K C_2 & C_1 Y + D_{12}\widehat{C}_K & D_{11}+D_{12}D_K D_{21} & -\gamma I \end{bmatrix} < 0 \tag{6}$$

In such case, a gain-scheduled controller of the form (5) is readily obtained with the following two-step scheme:

— *solve for* N, M, *the factorization problem*

$$I - XY = NM^T .$$

— *compute* A_K, B_K, C_K *with*

$$A_K = N^{-1}(X\dot{Y} + N\dot{M}^T + \widehat{A}_K - X(A - B_2 D_K C_2)Y - \widehat{B}_K C_2 Y - X B_2 \widehat{C}_K)M^{-T} \tag{7}$$

$$B_K = N^{-1}(\widehat{B}_K - X B_2 D_K) \tag{8}$$

$$C_K = (\widehat{C}_K - D_K C_2 Y)M^{-T} . \tag{9}$$

Note that since all variables are involved linearly, the constraints (6) constitute an LMI system. This system is, however, infinite due to its dependence on θ ranging over Θ. Using the Projection Lemma, detailed in [9], the controller variables can be eliminated, leading to a characterization involving the variables X and Y, only. This is presented in the next theorem.

Theorem 3.2 (Projected Solvability Conditions [5]) *Consider the LPV plant governed by (3), with parameter trajectories constrained by (4) and the assumption* **(A1)** *in force. There exists a gain-scheduled output-feedback controller (5) enforcing internal stability and a bound* γ *on the* L_2 *gain of the closed-loop system (3) and (5), whenever there exist parameter-dependent symmetric matrices* $Y(\theta)$ *and* $X(\theta)$ *such that for all* θ *in* Θ *the following infinite-dimensional LMI problem holds,*

$$\left[\begin{array}{c|c} \mathcal{N}_X & 0 \\ \hline 0 & I \end{array}\right]^T \left[\begin{array}{cc|c} A^T X A - X & A^T X B_1 & C_1^T \\ B_1^T X A & -\gamma I + B_1^T X B_1 & D_{11}^T \\ \hline C_1 & D_{11} & -\gamma I \end{array}\right] \left[\begin{array}{c|c} \mathcal{N}_X & 0 \\ \hline 0 & I \end{array}\right] < 0 \tag{10}$$

$$\left[\begin{array}{c|c} \mathcal{N}_Y & 0 \\ \hline 0 & I \end{array}\right]^T \left[\begin{array}{cc|c} AYA^T - Y & AYC_1^T & B_1 \\ C_1 Y A^T & -\gamma I + C_1 Y C_1^T & D_{11} \\ \hline B_1^T & D_{11}^T & -\gamma I \end{array}\right] \left[\begin{array}{c|c} \mathcal{N}_Y & 0 \\ \hline 0 & I \end{array}\right] < 0 \tag{11}$$

$$\begin{bmatrix} X & I \\ I & Y \end{bmatrix} > 0. \tag{12}$$

where $\mathcal{N}_X$ and $\mathcal{N}_Y$ designate any bases of the null spaces of $\left[\begin{array}{cc} C_2 & D_{21} \end{array}\right]$ *and* $\left[\begin{array}{cc} B_2^T & D_{12}^T \end{array}\right]$, *respectively.*

Note again that the characterization above is an infinite-dimensional LMI problem. It can be turned into a conventional LMI problem by a gridding of the parameter space Θ and by selecting basis functions for the matrices $X(\theta)$ and $Y(\theta)$ [8, 5]. This will be discussed more in-depth in the launcher application below. Also, when the matrix-valued functions $X(\theta)$ and $Y(\theta)$ are determined, one can use explicit formulas to compute the controller data (5) as functions of the scheduling variables θ. This allows online implementation of the controller as required by the gain-scheduling task. The reader is referred to [5] for more details on the controller construction.

4 The Cross Standard Form (CSF)

The CSF, previously detailed in [4] for continuous-time systems, is defined in this section for discrete-time systems. The CSF is based on an LQG controller structure or more generally on compensators involving a state observer (with an estimation gain K_f), a state feedback (with a gain K_c) and a dynamic Youla's parameter $Q(z)$. In discrete-time, one can distinguish 2 LQG structures : the predictor structure and the estimator structure (see [10] for more details). The discrete predictor LQG structure, and the Youla parameterization of all stabilizing controllers based on it, are analogous to the continuous-time case. All the results presented in this paper concerns the discrete estimator LQG structure. The structure of a such controller is depicted in Figure 1. Note that the direct feed-through D is ignored for simplicity. Also recall that this structure allows to parameterize all stabilizing controllers. The authors in [10] proposed a procedure to compute the parameters K_c, K_f and $Q(z)$ which characterize this structure from a controller $K(z)$ of arbitrary order n_K and a system $G(z)$ of order n.

The plant $G(z)$ is defined by the general state-space representation (n states with $n \leq n_K$, m inputs, p outputs) :

$$\left[\begin{array}{c} x_{k+1} \\ \hline y_k \end{array}\right] = \left[\begin{array}{c|c} A & B \\ \hline C & D \end{array}\right] \left[\begin{array}{c} x_k \\ \hline u_k \end{array}\right] \tag{13}$$

The state-space representation of the controller $K(z)$ associated with this structure (Figure 1 and considering the direct feed-through D) reads :

$$\left\{\begin{array}{ll} \hat{x}_{k+1} & = A\hat{x}_k + Bu_k + AK_f(y_k - C\hat{x}_k - Du_k) \\ x_{Q_{k+1}} & = A_Q x_{Q_k} + B_Q(y_k - C\hat{x}_k - Du_k) \\ u_k & = -K_c\hat{x}_k + C_Q x_{Q_k} + (D_Q - K_cK_f)(y_k - C\hat{x}_k - Du_k) \end{array}\right. \tag{14}$$

where A_Q, B_Q, C_Q and D_Q are the 4 matrices of the state-space realization of $Q(z)$ associated to the state vector x_Q.

Proposition 4.1 *The CSF, $P_p(z)$, associated with the compensator defined by (14), such that :*

$$F_l(P_p(z), K(z)) = 0 \tag{15}$$

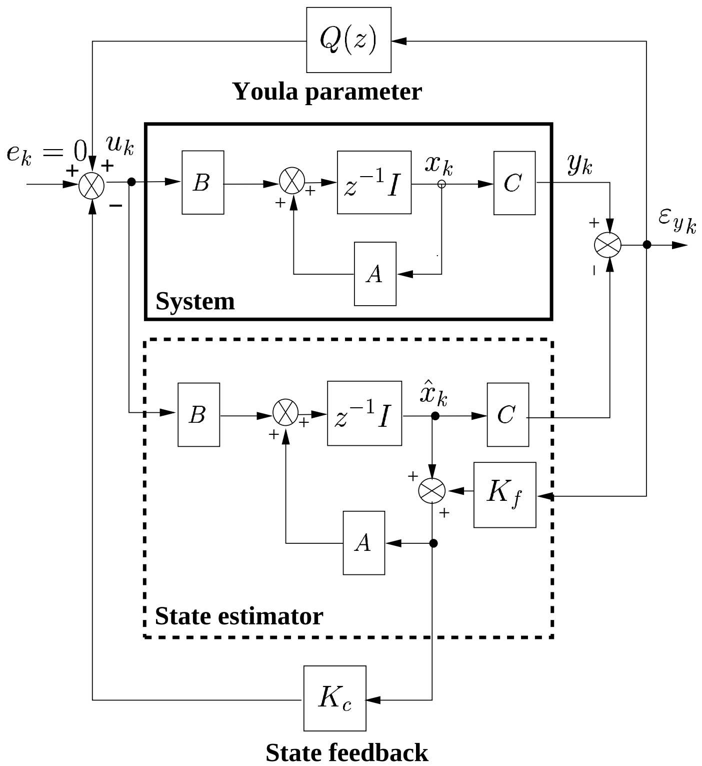

FIGURE 1: The discrete YOULA parameterization on the estimator LQG structure.

reads :

$$P_p(z) := \left[\begin{array}{cc|c|c} A & 0 & AK_f & B \\ 0 & A_Q & B_Q & 0 \\ \hline K_c & -C_Q & -D_Q + K_cK_f & I_m \\ \hline C & 0 & I_p & D \end{array}\right]. \tag{16}$$

Proof : See [11] for the discrete-time version or [4] for the continuous-time version.

□

Practical use : This result can be considered as a generalization, for H_2 and H_∞ criteria and for dynamic LQG output feedbacks, of the solution to the *LQ inverse* problem, extensively discussed in the Sixties and Seventies and which consisted in finding the LQ cost whose minimization restores a given state feedback. This CSF used as such is not of interest since it is necessary to know gains K_c and K_f and the Youla parameter $Q(z)$ to set up the problem $P_p(z)$ and to finally find the initial augmented LQG compensator. On the other hand, from an arbitrary compensator satisfying some time-domain specifications, one can compute an observer-based realization (i.e. K_c, K_f and $Q(z)$) of this compensator using the technique in [10]. The CSF is then immediately useful to initialize a standard setup which will be completed by dynamic weightings to take into account frequency-domain specifications.

5 Launcher control problem

5.1 Description

This application considers the launcher inner control loop.

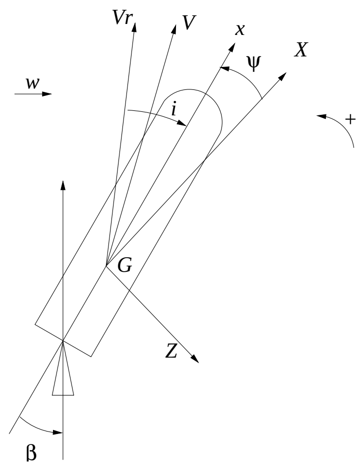

FIGURE 2: Launcher simplified representation.

According to Figure 2, we will use the notation :
— G : the center of gravity,
— i : the launcher angle of attack,
— ψ : the deviation angle around axis with respect to the guidance attitude reference,

— V and V_r : respectively the absolute and the relative velocities,
— w : the wind velocity,
— β : the thruster deflection angle.

The rigid model strongly depends on 2 uncertain dynamic parameters A_6 (aerodynamic efficiency) and K_1 (thruster efficiency).
From Figure 2 and under small angle assumption, one can derive the angle of attack equation :

$$i = \psi + \frac{\dot{z} - w}{V} \tag{17}$$

where $\dot{z}$ represents the lateral drift rate.

The discrete-time validation model considered in this paper, that is the full-order model $G_f(z)$, is characterized by the rigid dynamics , the thrusters dynamics, the sensors and the first 5 bending modes. The launcher is aerodynamically unstable. The characteristics of bending modes are uncertain. The parameters are kown as continuous time functions along the flight envelope of the launcher.

5.2 Objectives

The available measurements are the attitude angle (ψ) and the velocity ($\dot{\psi}$). The control signal is the thruster deflection angle β. Launcher control objectives for the whole atmospheric flight phase are as follows :

— performance with respect to disturbances (wind). The angle of attack peak, in response to the typical wind profile $w(t)$ (depicted in dashed plot in Figure 3), must stay into a narrow band ($\pm\, i_{max}$),
— closed-loop stability with sufficient stability margins. This involves constraints on the rigid mode but also on the flexible modes. In fact, the first flexible mode is "naturally" phase controlled (collocation between sensors and actuator) while the other flexible mode must be gain controlled (roll-off). So, the peaks associated with the flexible mode (except for the first) on the frequency response of the loop gain ($L(s) = K(s)G(s)$) must stay below a specified level X_{dB} for any parametric configurations (see Figure 7 as an example). From the synthesis point of view, the flexible modes are not taken into account in the synthesis model. But a roll-off behavior with a cut-off frequency between the first and the second flexible modes must be specified in the synthesis,
— robustness with respect to parameter uncertainties. This concerns both rigid (aerodynamics, propulsion, position of center of mass, inertia) and bending modes.
— one sampling period of delay margin.

All the objectives must be achieved for all configurations in the uncertain parameter space (22 uncertain parameters), particularly in some identified worst cases. In this paper, the robustness analysis is limited to these worst cases as the experience shown they are quite representative of the robustness problem. A more complete μ-analysis on stationnary launcher control problem is presented in [12].

6 Design of the LTI controller for the launcher

First of all, we will be interested in the stationnary launcher control design. For the different point of synthesis the method will be always the same. The approach we propose to satisfy all these objectives proceeds in 2 steps: the first one aims to satisfy time-domain specification (angle of attack constraint) and the second one is a H_∞ synthesis based on the CSF allowing the frequency-domain specifications (roll-off, stability margins) to be met.

The models used for the synthesis are discrete models including a zero-order hold. The computation of the first step of the synthesis is directly derived from the continuous-time synthesis [4].

6.1 First synthesis: non conventional LQG/LTR synthesis

6.1.1 State feedback on the rigid model

The rigid problem is characterized by 2 controlled outputs i and $\dot{z}$, 2 measurements ψ and $\dot{\psi}$, 1 control signal β and 1 exogenous input w (disturbance). This standard problem reads:

$$\begin{bmatrix} \dot{x}^r \\ \hline i \\ \dot{z} \\ \hline \psi \\ \dot{\psi} \end{bmatrix} = \left[\begin{array}{c|c|c} A & B_1 & B_2 \\ \hline C_1 & D_{11} & D_{12} \\ \hline C_2 & D_{21} & D_{22} \end{array}\right] \begin{bmatrix} x^r \\ \hline w \\ \hline \beta \end{bmatrix} \tag{18}$$

Then, we compute the gain K_d such that the discrete control law $\beta_k = -K_d\, x^r_k$ minimize the following continuous-time LQ criterion:

$$J = \int_0^\infty \left(\alpha \dot{z}^2 + i^2 + r\beta^2\right) dt \tag{19}$$

The discrete-time model can be written as $x^r_{k+1} = A_d x^r_k + B_{2_d}\beta_k$. The model and the performance index are discretized by taking into account the zero-order hold at the input β_k and are computed using the Van Loan's Formula [13].
In the sequel, we adopt the notation:

$$K_d = [K_\psi,\ K_{\dot{\psi}},\ K_{\dot{z}}]. \tag{20}$$

The gain K_d can be used to built a servo-loop of the measured variable ψ, that is:

$$\beta_k = K_\psi(\psi_{ref_k} - \psi_k) - K_{\dot{\psi}}\dot{\psi}_k - K_{\dot{z}}\dot{z}_k \tag{21}$$

where ψ_{ref_k} is the input reference.

6.1.2 Augmented state with wind dynamic

The wind dynamics is modelled by a stable filter and is then discretized with the zero-order hold method:

$$w_{k+1} = A_w w_k + \tilde{w}_k\ .$$

This rough model introduces a new tuning parameter A_w. The discrete-time augmented problem corresponding to the state vector $x^a = [x^r,\ w]^T$ then reads:

$$\left[\begin{array}{c} x^a_{k+1} \\ \hline i_k \\ \dot{z}_k \\ \hline \psi_k \\ \dot{\psi}_k \end{array}\right] = \left[\begin{array}{cc|c|c} A_d & B_{1_d} & 0 & B_{2_d} \\ 0 & A_w & 1 & 0 \\ \hline C_1 & D_{11} & 0 & D_{12} \\ \hline C_2 & D_{21} & 0 & D_{22} \end{array}\right] \left[\begin{array}{c} x^a_k \\ \hline \tilde{w}_k \\ \hline \beta_k \end{array}\right] = \left[\begin{array}{c|c|c} A^a_d & B^a_{1_d} & B^a_{2_d} \\ \hline C^a_1 & 0 & D_{12} \\ \hline C^a_2 & 0 & D_{22} \end{array}\right] \left[\begin{array}{c} x^a_k \\ \hline \tilde{w}_k \\ \hline \beta_k \end{array}\right] \qquad (22)$$

with: $B_{1_d} = \int_0^{T_s} e^{A\eta} B_1\, d\eta$.

To compute the new state feedback gain K^a_d associated with the state x^a, we consider the equation (21) where ψ_{ref_k} is computed, via the angle of attack equation (17), to cancel this angle of attack, that is:

$$\psi_{\mathrm{ref}_k} = \frac{w_k - \dot{z}_k}{V}.$$

Then, the term $\frac{\dot{z}_k}{V}$ is ignored because it can introduce unstabilizing couplings in the lateral motion. Finally, the gain K^a_d is obtained as:

$$K^a_d = \left[\ K_d \quad -\tfrac{K_\psi}{V}\ \right]. \qquad (23)$$

Following this procedure, we ensure that the LQ state feedback closed-loop dynamics are stable and satisfy:

$$\mathrm{spec}(A^a_d - B^a_{2_d} K^a_d) = \mathrm{spec}(A_d - B_{2_d} K_d) \cup \mathrm{spec}(A_w)$$

6.1.3 Kalman's filter with LTR tuning

To compute the gain G^a_d of the Kalman's filter on the augmented model (A^a_d, $B^a_{2_d}$, C^a_2, D_{22}), we consider an LTR tuning based on the continuous one (see also [4]). That is, the state noise is composed of 2 disturbing signals: one on the wind model input ($\tilde{w}$) and one on the control input β through a gain $\sqrt{\rho}$ (LTR effect):

$$W = \begin{bmatrix} \rho B_2 B_2{}^T & 0 \\ 0 & I \end{bmatrix} \quad \text{and} \quad V = v \begin{bmatrix} 1 & 0 \\ 0 & \omega_f^2 \end{bmatrix}.$$

W and V are the covariance matrices of continuous-time noises for the state vector (x^a) and for the measurement vector ($[\psi,\ \dot{\psi}]^T$), respectively. Therefore the Kalman filter tuning depends on 3 parameters: ρ (LTR weighting), v (measurement to state noise ratio) and $\omega_f\,(rd/s)$ (rate to position measurement noise ratio). ω_f represents the pulsation beyond which it is better to integrate the rate measurement $\dot{\psi}$ to estimate the position $\hat{\psi}$ than to use the measurement position ψ directly.

This non conventional LQG/LTR design yields a compensator $K_1(z)$ defined by the gains K^a_d and G^a_d and the four matrix of the augmented model (A^a_d, $B^a_{2_d}$, C^a_2, D_{22}).

The results obtained so far are presented in Figures 3 and 4.

We observe in Figure 3 that the performance requirements (angle of attack) are quite satisfied for all worst cases. In Figure 4, one can also note that the template for low frequency stability margins is satisfied (depicted in Figure 4 with the vertical line on the first critical

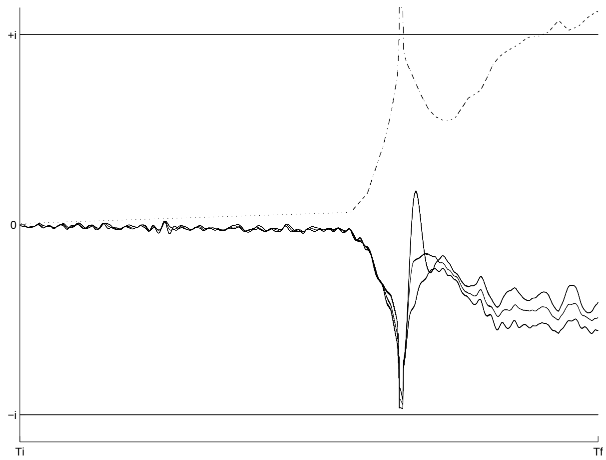

FIGURE 3: angle of attack $i(t)$ (solid) and wind profile $w(t)$ (dashed).

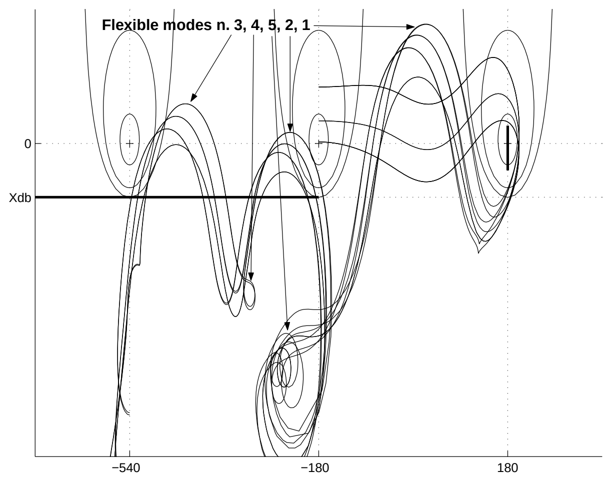

FIGURE 4: $K_1(z)G_f(z)$: Nichols's plots for parametric worst cases.

point on the right-hand side) and the first flexible mode stays away between two critical points for all worst cases (phase control). But the roll-off effect is not strong enough: the template for gain margins about flexible modes number 2 and 3 (depicted on Figure 4 with the horizontal line at $X\,dB$) is not satisfied for all worst cases. We can also observe that the flexible modes 4 and 5 are aliasing with respect to half sampling frequency and are not significant.

6.2 Second synthesis : H_∞ synthesis using CSF for frequency-domain specifications

In order to satisfy this last frequency domain requirement (template for gain margins around flexible modes number 2 and 3), we now perform an H_∞ synthesis with the standard problem depicted in Figure 5 :

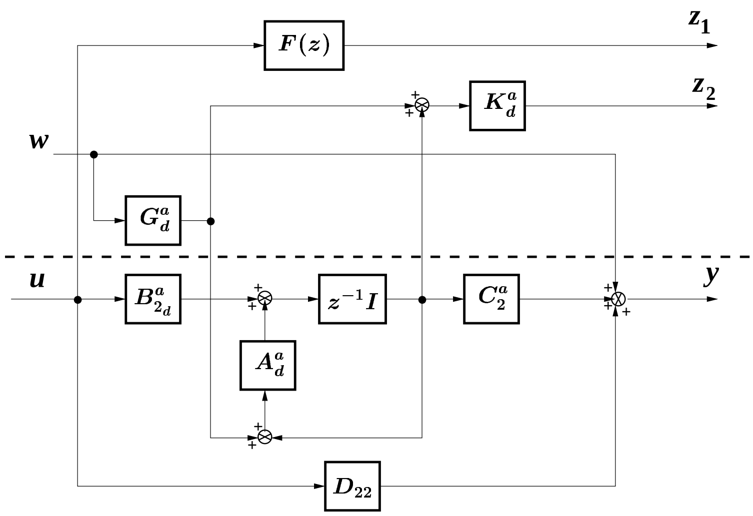

FIGURE 5: $P_f(z)$: setup for the final H_∞ synthesis.

This standard problem can be described as follows :

— between inputs w and u and outputs z_2 and y, we recognize the CSF presented in section 4 which will inflect the solution towards the previous pure performance compensator (LQG/LTR design),

— the output z_1 is introduced to specify the roll-off behavior with a filter $F(z)$.

Then, the H_∞ synthesis provides a 6th-order compensator $K_2(z)$. Analysis results are displayed in Figures 6 and 7. In Figure 6, we can see that the performance specifications are still met, and in the Nichols plot (Figure 7). Also stability margins are good enough for all worst cases and the roll-off behavior is quite satisfactory.

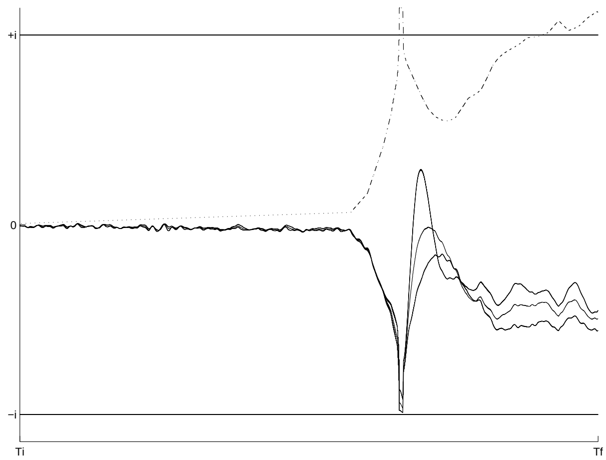

FIGURE 6: angle of attack $i(t)$ (solid) and wind profile $w(t)$ (dashed) with second controller.

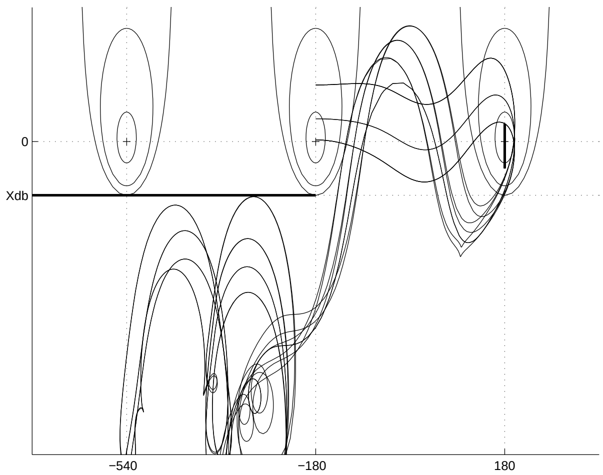

FIGURE 7: $K_2(z)G_f(z)$: NICHOLS plot for parametric worst cases with second controller.

We used the same procedure to compute the LTI controller for the whole atmospheric flight phase. We can see on Figure 8 that for each point the LTI controller achieved the stationnary specification.

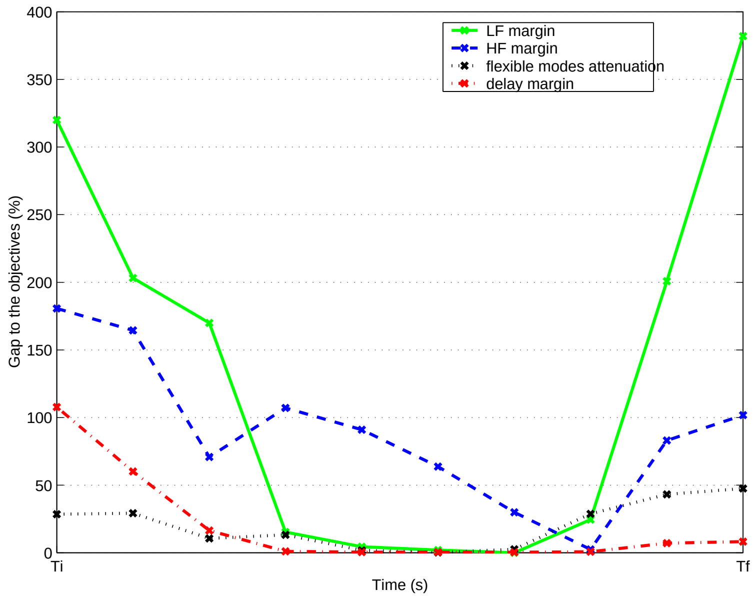

FIGURE 8: Specification balance graph w.r.t time for LTI compensators.

7 Linear Time Varying Launcher Control

We consider a set of synthesis points and construct the LTI standard problem for each of theses points using the previous approach. We compute the LTV problem of control (see equation 3, where $\theta = t$) through a linear interpolation of the LTI standard problems. Now, we must choose a functional dependence for the Lyapunov functions solution of the LMI constraints (10-12).

The rigid dynamic is naturally defined by 6 time functions [14] : the aerodynamic coefficients A_6 and K_1, the velocity V, and the parameters of the drift equation a_1, a_2 and a_3. So, the functional dependence (24) of X and Y is chosen to duplicate the natural dependancy of the rigid launcher :

$$\begin{array}{l} X(t) := X_0 + A_6 X_{A_6} + K_1 X_{K_1} + V X_V + a_1 X_{a_1} + a_2 X_{a_2} + a_3 X_{a_3} \\ Y(t) := Y_0 + A_6 Y_{A_6} + K_1 Y_{K_1} + V Y_V + a_1 Y_{a_1} + a_2 Y_{a_2} + a_3 Y_{a_3} \end{array} \quad (24)$$

To evaluate the possible distorsions of the performance, we compute the H_∞ norm on a very dense time-domain gridding. The Figure 9 displays the evolution of γ. On this Figure, we have also represented the H_∞ norm for the controller obtained as a linear interpolation of the LTI compensators.

The evolution of the singular value of $K_{LPV}(z, t)$ with respect to time t is depicted in Figure 10. We can note that the reponse is very smooth.

Figure 11 depicts the evolution of the stability margins during the whole atmospheric flight. We represent the variation in percent with respect to time t the desired margins (corresponding to the templates in the Nichols chart) : the low frequency gain margin, the high frequency gain margin, the attenuation of the flexible modes below X_{dB} and the delay margin.

Figure 12 depicts the time-domain simulation for the whole atmospheric flight.

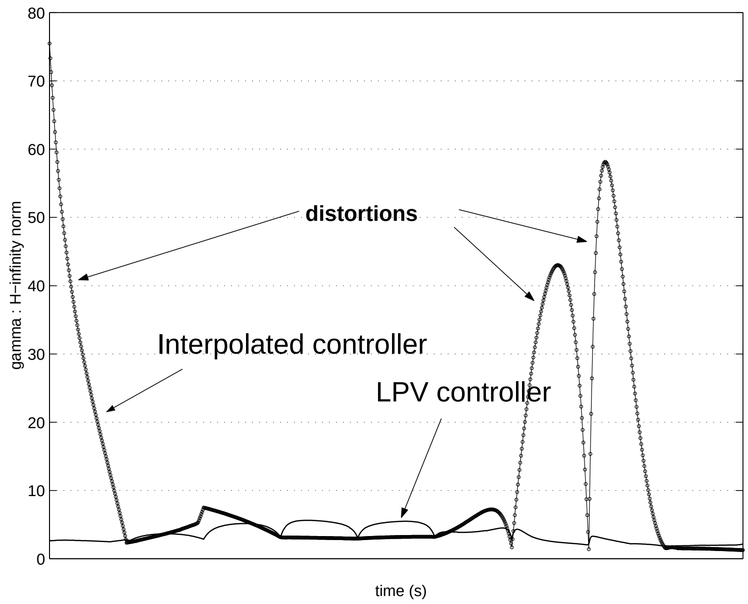

FIGURE 9: H_∞ performance.

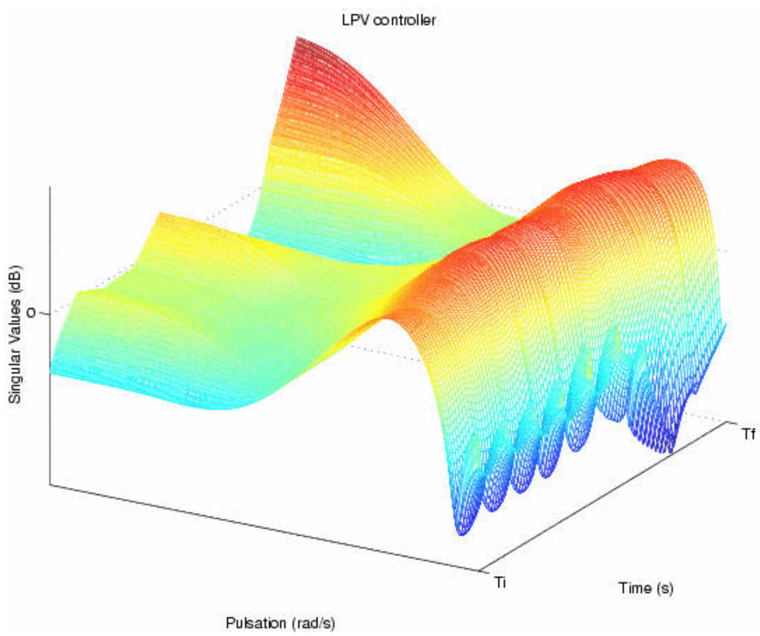

FIGURE 10: Singular value w.r.t time.

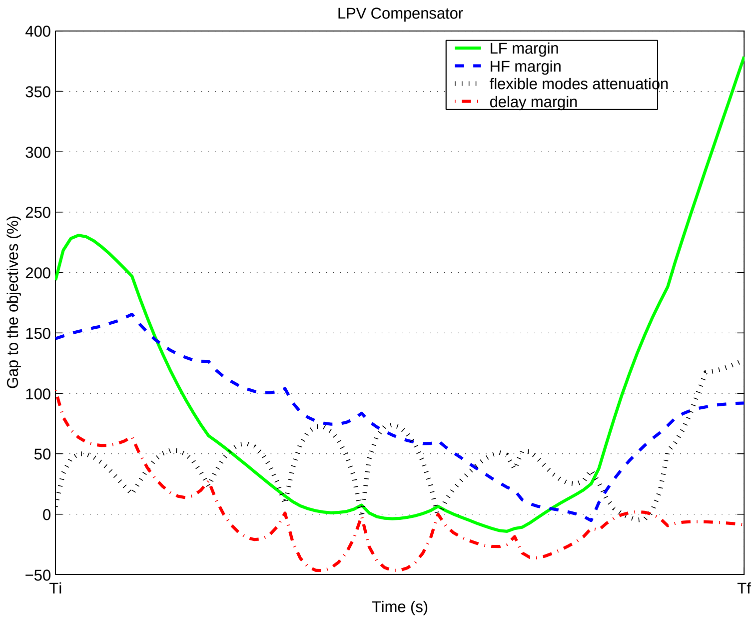

FIGURE 11: Specification balance graph w.r.t time.

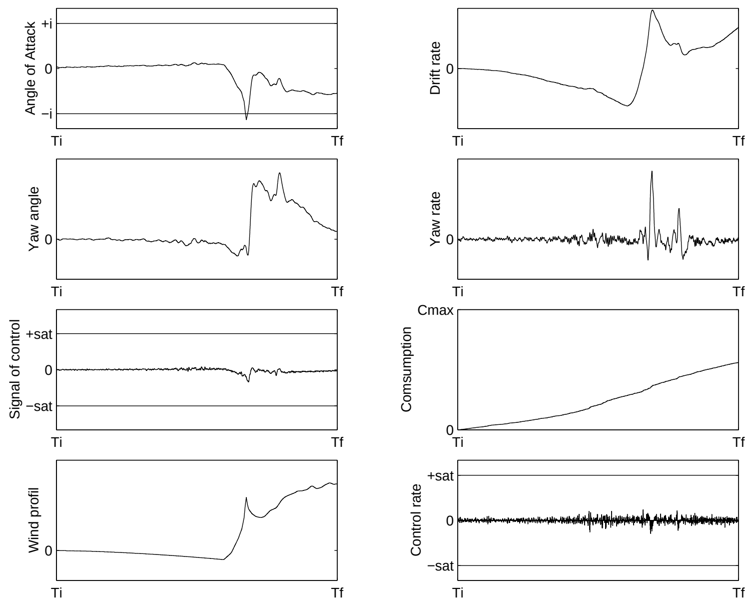

FIGURE 12: Time simulation.

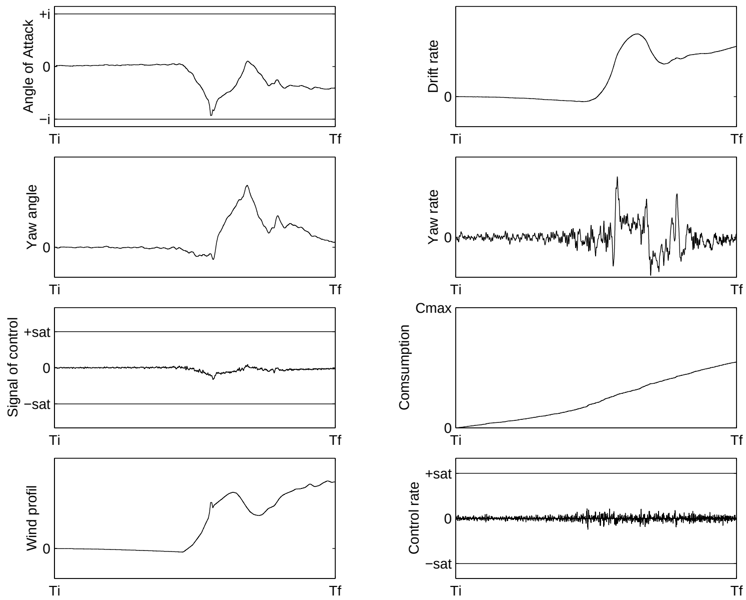

FIGURE 13: Time simulation (other wind profil).

8 Acknowledgements

This work has been carried out in collaboration with EADS/Launch Vehicles and CNES-DLA (French Space Agency).

Références

[1] S. Mauffrey and M. Scholler. Non-stationary $\mathcal{H}_\infty$ control for launcher with bending modes. In *14 Th. Symposium on Automatic Control in Aerospace*, Séoul, 1998. IFAC.

[2] B. Clément and G. Duc. A multi-objective control algorithm : Application to a launcher with bending modes. In *18th IEEE Mediterranean Conference on Control and Automation*, Patras, 17-19 July 2000.

[3] B. Clement, G. Duc, S. Mauffrey, and A. Biard. Gain scheduling for an aerospace launcher with bending modes. In *15th IFAC Symposium on Automatic Control in Aerospace*, Bologna, 2-7 September 2001.

[4] O. Voinot, D. Alazard, A. Piquereau, and A. Biard. A robust multi-objective synthesis applied to launcher attitude control. In *15th IFAC Symposium on Automatic Control in Aerospace*, Bologna, 2-7 September 2001.

[5] P. Apkarian and R. J. Adams. Advanced Gain-Scheduling Techniques for Uncertain Systems. *IEEE Trans. on Control System Technology*, 6(1) :21–32, january 1998.

[6] G. Becker. Parameter-Dependent Control of an Under-Actuated Mechanical Sys= tem. In *Proc. IEEE Conf. on Decision and Control*, LA, 1995.

[7] G. Becker. Additional Results on Parameter-Dependent Controllers for LPV S= ystems. In *IFAC World Congress*, pages 351–356, San Fransisco, USA, 1996.

[8] F. Wu, X. Yang, A. Packard, and G. Becker. Induced L_2-Norm Control for LPV System with Bounded Paramet er Variations Rates. In *Proc. American Control Conf.*, pages 2379–2383, Seattle, Wa., 1995.

[9] P. Gahinet and P. Apkarian. A Linear Matrix Inequality Approach to H_∞ Control=. *Int. J. Robust and Nonlinear Control*, 4(4) :421–448, 1994.

[10] D. Alazard and P. Apkarian. Exact oberserver-based structures for arbitrary compensators. *Internationnal Journal of Robust and Non-Linear Control*, 9 :101–118, 1999.

[11] O. Voinot, D. Alazard, P. Apkarian, S. Mauffrey, and A. Biard. A discrete time robust multi-objective synthesis applied to launcher attitude control. *Submitted for publication*, 2001.

[12] N. Imbert. Robustness analysis of a launcher attitude controller via μ-analysis. In *15th IFAC Symposium on Automatic Control in Aerospace*, Bologna, 2-7 September 2001.

[13] C. F. Van Loan. Computing integras involving the matrix exponential. *IEEE Transactions on Automatic Control*, AC-23(3) :395–404, 1978.

[14] B. Clément. *Synthèse multi-objectifs et séquencement de gains : Application au pilotage d'un lanceur spatial.* Thèse de Doctorat de l'Université Paris XI Orsay, 2001.